J. Meas. Sci. Instrum., 2021, 12(3): 331-339 http://xuebao.nuc.edu.cn
DOI: 10.3969/j.issn.1674-8042.2021.03.011 jmsi@nuc.edu.cn

Channel characteristics analysis of train-to-train wireless communication

GAO Yunbo, TIAN Zhiyu, LI Maoqing, YUE Lili, YAN Lixia, CHENG Xuan

(*School of Automation and Electrical Engineering, Lanzhou Jiaotong University, Lanzhou 730070, China*)

Abstract: Train-to-train (T2T) communication can provide protection for existing train-to-ground private network communication, and its channel characteristics directly affect the application of upper-layer communication technologies. In this study, based on the spatial distribution structure of railway operation scenarios and Fresnel zone theory, we propose a frequency allocation scheme for direct communication between tracking trains in flatland and long straight tunnel scenario. Then we use the estimation method of radio wave attenuation caused by rainfall to analyze the large-scale path loss fading of multi-band wireless channels. Furthermore, we derive the calculation equation of max Doppler frequency shift suitable for T2T communication and describe the multipath wave in the tunnel by ray tracing method to analyze small-scale fading. Simulation analysis shows that the Doppler shift value of T2T communication low frequency band is significantly lower than the frequency shift value of the train-to-ground communication under the same speed conditions.

Key words: train-to-train communication; Fresnel zone; long straight tunnel; wireless channel; Doppler frequency shift calculation

0 Introduction

The railway-specific mobile communication network increases the signal strength and communication distance by covering base stations on a large scale along the line, but the stability of communication equipment will be affected by extreme weather[1]. In order to ensure the real-time and accuracy of the high-speed railway mobile communication system and meet the development needs of the next generation train control system, train-to-train (T2T) communication came into being. It takes trains as core, minimizes the number of train-track side equipment, and realizes direct communication between tracking trains without the participation of base stations. The usage of T2T is to assist train-to-ground wireless communication network-based train control systems to achieve direct communication between trains in the event of a failure, which can expand collision hazard detection and broadcast early warnings, thereby improving the safety of train operation. Therefore, it is necessary to complete the analysis of the characteristics of the dedicated channel to lay the foundation for the design and network planning of far-distance communication system.

In recent years, scholars have studied the communication method of the auxiliary for global mobile communications system for railway (GSMR) and its channel characteristics. In terms of short-distance communication, Ref.[2] presentsdirect communication between subway trains at a travel speed of 80 km/h based on radio frequency technology, whose straight line covers a distance of 1.6 km. Lehner et al. utilized the trunk mode of the terrestrial trunked radio (TETRA) to achieve 4 km temporary communication between trains, and evaluated the channel characteristics of each scenario through the classic cellular network loss model[3], but they did not propose a corresponding channel model for the T2T application scenario. In Ref.[4], in the case where the radio wave propagation area is blocked by an open-air platform and bushes, automatic coupling between trains is achieved based on the millimeter wave Q-band. In terms of long distance communication, Liu et al. took other track-trains as transmission relays to achieve direct communication between the same track trains, but its

Received date: 2020-05-04

Foundation items: National Natural Science Foundation of China (No. 61763023); Lanzhou Jiaotong University—Tianjin University Innovation Fund (No. 20180519)

Corresponding author: GAO Yunbo (13370901@qq.com)

application scenarios are only limited to large stations and marshalling stations[5]. Chen et al. used ultra short wave to realize train-mounted ad hoc networks, and provided the station and interval communication link loss budget models[6]. Unterhuber et al. measured the small-scale fading characteristics of radio waves caused by Doppler spreading and multipath delay spreading in high-speed railway scenes, and introduced large-scale models of path loss in rural, suburban, and tunnel environments, but they did not consider extreme weather factors and specific frequency-bands selection scheme[7]. Mohammad et al. proposed that the Doppler frequency shift is a key factor affecting high-speed railway wireless communication systems, and they used improved Fitz algorithm to estimate the instantaneous value of the Doppler frequency shift, but the single-mobile computing model taking fixed base stations and trains as mobile body was still used[8]. He et al. used a ray tracer to verify the radio wave propagation in the tunnel, and analyzed the channel characteristics under the influence of multipath effects[9]. The results show the dependence of radio wave propagation characteristics on the system operating frequency, antenna polarization, and tunnel size.

In our work, we summarize the special operating scenarios of high-speed railways such as U-shaped groove, stations, tunnels, and viaducts according to the spatial structure. Combining Fresnel zone theory, we determine the communication distance and operating frequency band that are suitable for the above scenarios and serve to the wireless channel characteristic analysis. Additionally, considering the influence of weather on the selected frequency-band, its feasibility is verified through large-scale electromagnetic wave propagation theory. Furthermore, we derive the calculation equation of Doppler frequency shift under the relative motion of the train (dual mobile end), and verify the superiority of the T2T frequency shift value over the train-ground system at the same speed level. Finally, the ray tracing method is used to simulate multipath waves in the tunnel, and under different reflection conditions, the small-scale fading characteristics of wireless channels are simulated and analyzed.

1 System parameters

1.1 Communication range

Selection of working frequency should meet the following standards:

1) $D \geqslant d$, where D is the effective line-of-sight distance for electromagnetic wave propagation, and d is the distance between the receiver and the transmitter, that is, the communication distance.

2) In order to establish a reliable communication link, communication distance should be greater than the maximum emergency braking distance of the train.

The emergency braking distance of high-speed railway trains on straight roads is in accordance with Article 169 of the latest revised "Technical Regulations for Railway Technology", which takes the maximum allowable value[10], as shown in Table 1.

Table 1 Train braking distance

Project	Value			
Brake first speed (km/h)	350	300	250	200
Braking distance (m)	6 500	3 800	3 200	2 000

In order to meet the reliability of communication link established at the maximum initial braking speed of train, and to ensure consistency of communication distance in each scene, the line-of-sight propagation distance needs to be calculated. As shown in Eq. (1), h_t and h_r indicate heights of the transmitting and receiving antennas from the ground, respectively, generally 4.2 m[6] is taken. Line-of-sight by calculated with communication distance D is 14.6 km.

$$D = 3.57(\sqrt{h_t} + \sqrt{h_r}). \tag{1}$$

1.2 Working frequency

Radio waves can be divided into bands for communication occasions according to the wave length. The working frequency band of the current railway digital mobile communication system is about 900 MHz, while T2T mainly transmits train control key information such as location and speed, whose short message is about 150 bit[11], therefore, the low bandwidth could meet the transmission requirements. However, the high-speed railway operation scene is changeable, and low-speed propagation of radio waves in the tunnel will cause serious multipath effects. Therefore, T2T exclusive frequency allocation scheme must be established according to the spatial distribution structure of the railway operation scenarios.

Referring to Fresnel theory, the elliptical area

taking transmitter and receiver as the focus is the Fresnel zone, the extent to which area is blocked by obstacles determines the quality of communication. The radius of concentric circles of the Fresnel zone is calculated by

$$R_n = \sqrt{\frac{n\lambda d_1 d_2}{d_1 + d_2}}, \tag{2}$$

where d_1 and d_2 are the distances between the transmitter and receiver to the center of the cross-section of the Fresnel zone, respectively; n is the number of Fresnel zones; and λ is the wavelength. When $d_1 = d_2 = d/2$, the first Fresnel zone radius takes the maximum value.

When 80% of the first Fresnel region S is not blocked by obstacles, communication quality can be guaranteed, and the wireless link propagation space is considered as free space. Simultaneously, the ideal working frequency band in each scenario is obtained by calculating the occlusion area S' accoroding to

$$\frac{S'}{S} \leqslant 20\%. \tag{3}$$

Tunnel is an inner closed area. Compared with other scenes, the reflection, scattering of the radio waves on the top, bottom, and side walls will cause severe multipath delay expansion. The height of the antenna mounted on the compartment roof will affect the spatial distribution of the Fresnel zone, as shown in Fig. 1.

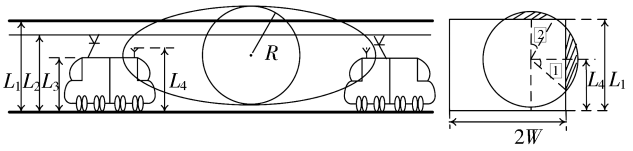

L_1: Tunnel height 7 150 mm L_2: Catenary height ⩾5 700 mm
L_3: Train height 3 889 m L_4: Antenna height 4 200 mm

Fig. 1 Spatial distribution of the first Fresnel zone in a double track tunnel

The ideal radius can be approximated by calculating the minimum cross-section blocking area in the Fresnel zone, the calculation process is

$$S' = \frac{2(\theta_1 + \theta_2)}{360}\pi R^2 - \frac{W}{2}\sqrt{R^2 - \left(\frac{W}{2}\right)^2} - (L_1 - L_4)\sqrt{R^2 - (L_1 - L_4)^2}. \tag{4}$$

When blocking is less than 20%, $R_{\max}$ is 3.8 m. Eq. (3) is used to calculate λ, and the lower limit of the selected frequency band is 34 GHz, which theoretically meets the maximum Fresnel zone coverage and reduces multipath effects in tunnel. The atmospheric window value of 35 GHz is preferred.

Except for shrubs, U-shaped groove and shallow cuts, and viaduct arms in the plain area, there are no obvious obstructions. The spatial distribution of Fresnel is shown in Fig. 2.

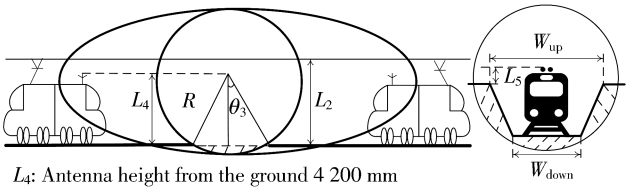

L_4: Antenna height from the ground 4 200 mm
L_5: Antenna distance U-shaped outer edge 2 000 mm

Fig. 2 Spatial distribution of the first Fresnel zone in the plain

Deep U-shaped groove will cause shadow fading, and at the same time, they will temporarily block the direct path. A large number of anti-scattered waves generated by steep walls will cause great fading to the signal. Route classification is shown in Table 2. The longer the selected frequency wavelength in this scenario, the larger the cross-sectional area of the Fresnel zone, and the smaller the relative occlusion area, that is, the lower the frequency, the stronger the diffraction ability, and the larger the Fresnel radius.

Table 2 Route classification

Width	Deep U-shaped groove			Shallow U-groove	
W_{up}/ (m)	58.30	55.26	49.77	48.38	50.24
W_{down}/ (m)	15.16	18.57	17.97	17.14	16.96

After selecting the value of the U-shaped groove, combining with the height of the CHR380B body, the actual occlusion area is calculated by

$$S' = \frac{2\theta_3}{360}\pi R^2 - L_5\sqrt{R^2 - (L_5)^2} - \frac{1}{2}(W_{up} + W_{down})(L_4 - L_5), \tag{5}$$

where $\theta_3 = \arccos(L_5/R)$. When the communication distance d is 6.5 km, the braking distance of the train with the initial braking speed of 350 km/h is satisfied, and $R_{\max}$ is 13.2 m. Substituting them into Eq. (2) to calculate λ, that is, the lower limit of the selected frequency band is 2.8 GHz, and this frequency belongs to the ultra high frequency radio frequency band.

1.3 Link budget

The link budget is an estimate of the path loss in the entire communication process since an accurate link budget is a prerequisite to overcome high losses. According to the actual operating status of the train, combined with the aforementioned calculation of the

working frequency band, when the two trains are running inside and outside in tunnel, respectively, the working frequency band is the millimeter wave *Q* band, and communication quality is extremely susceptible to extreme weather. Rainfall not only attenuates or depolarizes the millimeter wave signal, its scattering effect on millimeter waves will also cause mutual interference between detection systems. Hence, it is necessary to establish a large scale T2T path loss calculation model.

When calculating raindrop attenuation, refering to the distribution model of M-P raindrop spectrum, its shape is a sphere, and the size distribution is shown in Table 3.

Table 3 Raindrop size under different rainfalls

Weather	Rainfall (mm · h^{-1})	Raindrop diameter (mm)
Light rain	<10	0—1.50
Moderate rain	10—25	1.50—2.00
Torrential rain	25—50	2.00—2.25
Rainstorm	50—100	2.25—3.00
Heavy rain	100—200	3.00—3.25

According to Recommendation P. 838-3 of the International Telecommunication Union Radio Sector (ITU-R), the rain attenuation γ_R can be calculated from the power law relationship of the rainfall intensity R.

$$\gamma_R = kR^{\alpha}, \tag{6}$$

where the values of the coefficients k and α vary with the polarization mode of the antenna (vertical, horizontal), k can be expressed by k_{H} and k_{v}, and α can be expressed by α_{H} and α_{v}. According to measured values provided by ITU-R, some values are shown in Table 4, unit of frequency is GHz.

Table 4 Values of different frequencies k and α

f(GHz)	k_{H}	α_{H}	f	k_{H}	α_{H}
1	0.000 025 9	0.969 1	31	0.258 8	0.939 2
3	0.000 139 0	1.232 2	33	0.297 2	0.921 4
5	0.000 216 2	1.696 9	35	0.337 4	0.904 7
7	0.001 915 0	1.481 0	37	0.378 9	0.889 0
9	0.007 535 0	1.315 5	39	0.421 5	0.874 3
11	0.017 220 0	1.214 0	41	0.464 7	0.860 5
13	0.030 410 0	1.158 6	43	0.508 4	0.847 6
15	0.044 810 0	1.123 3	45	0.552 1	0.835 5
17	0.061 460 0	1.094 9	47	0.595 6	0.824 1
19	0.080 840 0	1.069 1	49	0.638 6	0.813 4
21	0.103 200 0	1.044 7	51	0.681 1	0.803 4
23	0.128 600 0	1.021 4	53	0.722 8	0.794 1
25	0.157 100 0	0.999 1	55	0.763 5	0.785 3
27	0.188 400 0	0.978 0	57	0.803 2	0.777 1
29	0.222 400 0	0.958 0	59	0.841 8	0.769 3

The values in Table 4 can fit the relationship curve between each frequency and the amount of rainfall attenuation. It can be seen from Fig. 3 that high frequency bands are more susceptible to rainfall than low frequency bands, with loss up to 35 dB/km.

The path loss of the ideal operating frequency band calculated above can be calculated according to the free space propagation model, but considering the actual operating environment, a corresponding model should be selected for different environments. Assuming the antenna has unity gain, the free-space path loss is

$$L_{\mathrm{free}}(\mathrm{dB}) = -10\left[\frac{\lambda^2}{(4\pi)^2 d^2}\right]. \tag{7}$$

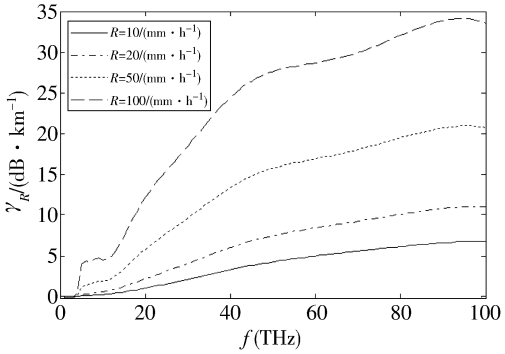

Fig. 3 Relationship between frequency and rainfall attenuation

In Ref. [12], the model was selected as the reference model after comparing the measured values with the Okumura-Hata. According to the measured analysis by the German Aerospace Agency, the model is also considered to be suitable for T2T communication,

$$\begin{cases} L_{\mathrm{urb}} = 69.55 + 26.16\lg f - 13.82\lg h_{\mathrm{t}} - \\ \qquad a h_{\mathrm{r}} + (44.9 - 6.55\lg h_{\mathrm{t}})\lg d, \\ L_{\mathrm{open}} = L_{\mathrm{urb}} - 4.78\lg^2 f + 18.33\lg^2 f - 40.94, \end{cases} \tag{8}$$

$$a(h_{\mathrm{r}}) = 3.2\lg^2(11.75h_{\mathrm{r}}) - 4.97 \quad (f \geqslant 400\ \mathrm{MHz}), \tag{9}$$

where f is the carrier frequency (MHz); L_{urb} and L_{open} are the path loss of cities and open areas (dB), and a (h_r) is the antenna height correction factor.

There are many reflection paths in the electromagnetic wave propagation path in the tunnel, a mix of line of sight (LOS) and non line of sight (NLOS) with the shadow fade[13], logarithmic path loss model after adding rainfall attenuation is shown in Eq. (10). The total path loss L_{sum} includes the basic path loss $L_{\mathrm{free}}(d_0)$, where d_0 is a fixed reference point distance. At any d, the path loss $L_{\mathrm{sum}}(d)$ at this position is a random normal logarithmic distribution, and χ_σ is a Gaussian random variable with zero mean.

$$L_{\text{sum}}(\text{dB}) = L_{\text{free}}(d_0) + 10\lg\frac{d}{d_0} + \chi_\sigma + \gamma_R d, \quad (10)$$

$$P_{\text{in}} = -174 + 10\lg B + F_{\text{N}} + R_{\text{SN}}, \quad (11)$$

where F_{N} is noise figure, and R_{SN} is bit signal-to-noise ratio.

Receiver sensitivity P_{in} is the minimum received signal strength for normal system operation (unit: dBm)[14]. In order to reliably receive multi-band signals, it should meet the requirements of each frequency band.

The typical noise figure of a millimeter wave receiver is 3 dB—6 dB, the effective bandwidth B is 10 kHz, and the R_{SN} is 4 dB. When the carrier frequency is 35 GHz, the receiver sensitivity is −127 dBm.

The frequency band in plain area is different from that in the tunnel, therefore, the path loss is different. As shown in Fig. 4, the loss of each model increases with distance, the maximum path loss in the plain area is about 145 dB. When the rainfall outside the tunnel is 10 mm/h and the two trains traveling inside and outside tunnel meet communication distance requirements, if f is 35 GHz is used, the maximum path loss is about 160 dB. If the transmission power is set properly, the receiver sensitivity can be matched with the aforementioned calculation value.

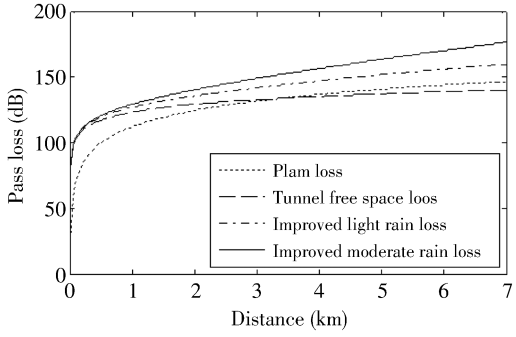

Fig. 4 Relationship between path loss and distance

2 Analysis of radio wave channel propagation characteristics

2.1 Doppler frequency calculation

As a carrier of radio wave propagation, wireless channel is developed around straight shot, diffraction, and scattering mechanisms. Doppler frequency shift f_{d}, as one of the factors affecting small-scale fading, reflects the change of the frequency value of the received signal caused by the path difference, and is closely related to the speed[15]. Traditional train-ground communication takes a ground base station as the electromagnetic wave emission source. There is an angle θ between the direction of signal incidence and the movement of the receiving point. The phase of the receiving point changes with the change of the moving distance, which affects the frequency change, that is,

$$f_{\text{d}} = f_0\frac{V}{c}\cos\theta. \quad (12)$$

Compared with the traditional cellular system, T2T transmitter and receiver are moving fast, thus the calculation model that uses a train as a mobile station and a fixed base station is no longer applicable. For high-speed trains with speeds ranging from 250 km/h to 350 km/h, to establish long distance direct-communication links between trains, the Doppler frequency shift estimation method needs to be improved.

In the line-of-sight communication range, the process of radio wave propagation is simplified to the communication application process for the mobile terminal of a periodic train, and the distance and speed changes within the period are used for derivation. Assuming that the interval at which the transmitter sends a communication request is T_0; the interval at which the receiver receives a communication request is T; the initial positions of the front and rear trains are at positions r and t, respectively, with X_1 apart; and the speeds are V_r and V_t; after T_0, trains arrive at t' and r', respectively, and the radio wave propagation speed is V. The two-train tracking operation process is shown in Fig. 5.

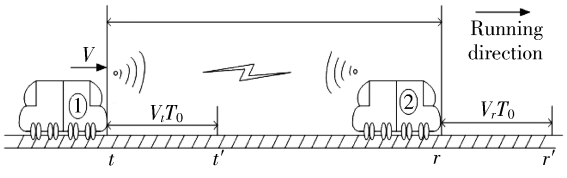

Fig. 5 Schematic diagram of procwss train tracking

The time when preceding train receives communication request for the first time is

$$t_1 = \frac{X_1}{V - V_r}, \quad (13)$$

after the interval T_0, the distance between the two becomes

$$X_2 = X_1 - (V_t - V_r)T_0. \quad (14)$$

When preceding train receives communication request for the second time, the time is

$$t_2 = T_0 + \frac{X_2}{V - V_r}, \quad (15)$$

thus the preceding train receives the communication request interval T is

$$T = t_2 - t_1 = \frac{V - V_t}{V - V_r} T_0, \tag{16}$$

and the frequency value f on the receiving end is

$$f = \frac{V - V_r}{V - V_t} f_0. \tag{17}$$

Finaly, we can get

$$f_d = f - f_0 = \frac{V_t - V_r}{V - V_t} f_0. \tag{18}$$

According to Eq. (18), the frequency shift value f_d of the two trains in relative motion can be obtained. When the two trains are relatively stationary, the max Doppler frequency shift value is zero.

2.2 Analysis of fading caused by Doppler spread

Train running speed determines the change trend of Doppler frequency shift value. For high-speed railways with a running interval of 3 min, the driver will drive according to the target-distance curve. The train will go through the stages of traction, cruise, inertia and braking. That is, the uniformly accelerated motion is transformed into a uniform motion. According to the actual operation of the train, including the station pick-up, stopping avoidance and interval tracking, the Doppler frequency shift range can be estimated through the following representative modes (V_1 = 300 km/h, V_2=350 km/h, a=0.5 m/s^2):

1) The front train starts from the station at the initial speed V_1 and accelerates uniformly to V_2, the following train travels in the section at a constant speed of V_2.

2) In the section, the front car travels at a constant speed of V_1, and the rear car accelerates at an initial speed of V_1 to a speed of V_2.

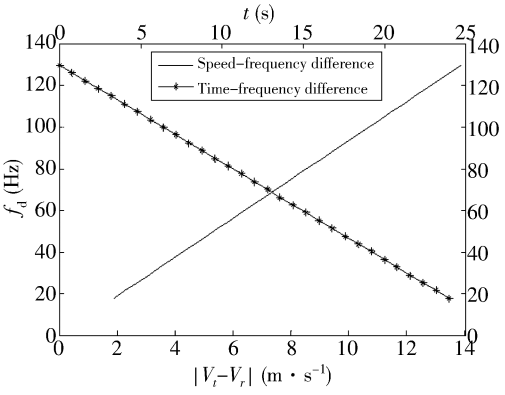

Fig. 6 Outbound train and interval running train establish communication

Case 1: As shown in Fig. 6, the two trains are gradually approaching, the source of the wave is close to the receiver, the number of waves received is greater than that sent by the transmitting end, that is, the frequency of the received signal is higher than that of the transmission, the frequency shift value increases and decreases over time.

Case 2: The two trains are gradually away, and the receiver is far away from the wave source. The number of waves received is less than that sent by the transmitting end, that is, the frequency of the received signal is lower than the transmission frequency. The Doppler frequency shift value increases over time, as shown in Fig. 7.

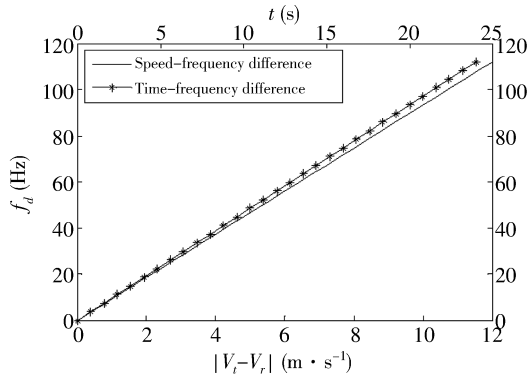

Fig. 7 Interval tracking train establishing communication

By estimating the frequency shift value, the linear relationship between the Doppler frequency shift and the train speed difference can be obtained. When the carrier frequency is 2.8 GHz, the speed difference is between 0 — 14 m/s, and the maximum Doppler frequency shift value is 130 Hz. Similarly, when the two trains travel inside and outside the tunnel, the carrier frequency is 35 GHz. This situation also belongs to interval tracking, and the maximum Doppler frequency shift value is 1.5 kHz. In summary, the f_d estimation results show that the Doppler shift value of T2T communication low-frequency band is significantly lower than the frequency shift value of the train-to-ground communication under the same speed conditions.

2.3 Statistical analysis of channel reference model

T2T channel is an end-to-end type, and its signal complex envelope correlation function $R_v(\Delta t)$ uses the time difference as a variable. The similarity between the superposition signal of each path at the receiving end caused by the multipath effect and the original signal can be expressed to reflect the change

of channel parameters, namely

$$R_v(\Delta t) = \sigma^2 J_0\left(\frac{2\pi}{\lambda}V_t \Delta t\right) J_0\left(\frac{2\pi}{\lambda}V_r \Delta t\right), \quad (19)$$

$$R_v(\Delta t) = \sigma^2 J_0\left(\frac{2\pi}{\lambda}f_{\mathrm{mr}} \Delta t\right) J_0\left(\frac{2\pi}{\lambda}f_{\mathrm{mt}} \Delta t\right), \quad (20)$$

where J_0 is the first-order Bessel zero-order function; σ^2 is the time average value of the received power; and f_{mt} and f_{mr} are the maximum frequency shift values at the transmitting and receiving ends, respectively, indicating that the Doppler effect of two carrier frequencies under different driving conditions[16]. It can be seen from Fig. 8 that the larger the frequency shift value, the faster the time domain convergence degree of the signal, and the more obvious the channel change. In order to reduce the multipath effect, the radio wave propagation in the tunnel needs to be analyzed.

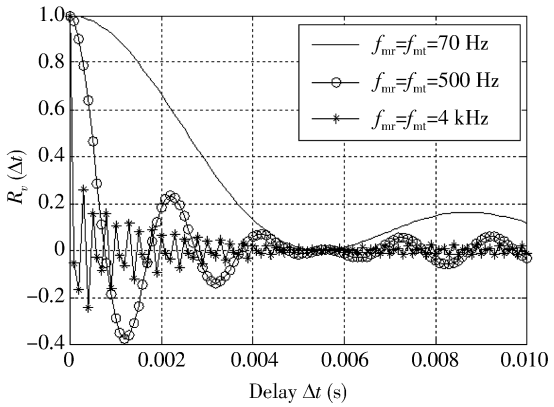

Fig. 8 Influence of Doppler shift on wireless channel

3 Multipath analysis in tunnel

3.1 Multipath reflections in tunnel

Multipath delay spread is one of the factors that affect small-scale fading. Because the distance of radio waves passing through each path is different, and the arrival time of reflected waves in each path is different, multipath fading in the tunnel is particularly serious. Thus, the ray tracing method[17] is used to analyze the signal power change of the radio waves in the tunnel that reach the receiving end after straight shot and reflected propagation, so as to grasp the relationship between the delay and the received power under different paths. The geometric model is shown in Fig. 9.

The received signal power at the receiving end is

$$P_{\mathrm{r}} = P_{\mathrm{t}}\left(\frac{\lambda}{4\pi}\right)^2 G_{\mathrm{t}}G_{\mathrm{r}} \times \left|\frac{\exp\left(\frac{-\mathrm{j}2\pi k}{\lambda}\right)}{k} + \sum_{i=1}^{q} R_i \frac{\exp\left(\frac{-\mathrm{j}2\pi k_i}{\lambda}\right)}{k_i}\right|, \quad (21)$$

where P_{t} is the transmission power, k_i is the propagation distance of different reflection paths, and R_i is the reflection coefficient of the ith reflected wave.

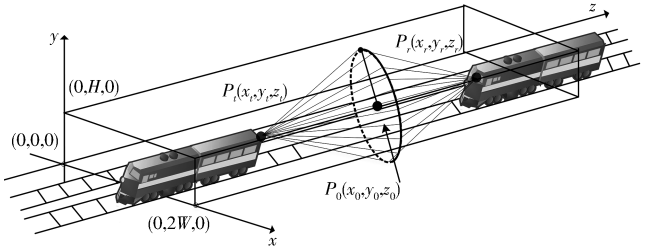

Fig. 9 Schematic diagram of geometric modeling in tunnel

$$R_i = R_{\mathrm{h}}\cos\theta_i + R_{\mathrm{v}}\sin\theta_i, \quad (22)$$

$$R_{\mathrm{h}} = \frac{-\varepsilon_{\mathrm{r}}\sin\theta_i + \sqrt{\varepsilon - \cos^2\theta_i}}{\varepsilon_{\mathrm{r}}\sin\theta_i + \sqrt{\varepsilon - \cos^2\theta_i}}, \quad (23)$$

$$R_{\mathrm{v}} = \frac{-\sin\theta_i - \sqrt{\varepsilon - \cos^2\theta_i}}{\sin\theta_) - \sqrt{\varepsilon - \cos^2\theta_i}}, \quad (24)$$

where θ_i is the incident angle of the ith reflected radio wave, and R_{h} and R_{v} are the horizontal and vertical polarization reflection coefficients of the antenna.

3.2 Millimeter wave reflection in Double line tunnel

Partners in our research group have completed the establishment of the reflection model of the top and bottom of the single-line tunnel[18]. On this basis, ray tracking method is used to conduct ray statistics for the rectangular double-line tunnel with a height of H and a width of $2W$. The reflected signal at the receiving end consists of the reflection from the top, bottom and side walls of the tunnel, as shown in Fig. 10.

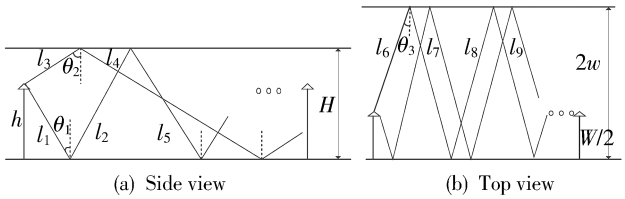

Fig. 10 Electromagnetic wave reflection diagram in tunnel

In the single odd-frequency reflection path at the top and bottom of the double-line tunnel, the ith reflection corresponds to $i+1$ reflection path, and the total length of the path k_i, therefore the included angle θ_i by reflection from the bottom and top can be expressed as

$$k_i = \sqrt{(2h + (i-1)H)^2 + d^2}, \quad (25)$$

$$\sin\theta_i = \frac{2h - (i-1)H}{k_i}. \quad (26)$$

Similarly, for even number of reflections, the total length of path k_i and the included angle θ generated by reflection through the bottom and top can be expressed as

$$k_i = \sqrt{(iH)^2 + d^2}, \tag{27}$$

$$\sin\theta_i = \frac{iH}{k_i}. \tag{28}$$

The total length k_i of the odd reflection path on the side wall and the included angle θ between the reflection path and the side wall of the tunnel become

$$k_i = \sqrt{(W + (i-1)2W)^2 + d^2}, \tag{29}$$

$$\sin\theta_i = \frac{W + (i-1)2W}{k_i}. \tag{30}$$

The even-number reflection path model of the side wall is calculated by

$$k_i = \sqrt{(2W + (i-1)2W)^2 + d^2}, \tag{31}$$

$$\sin\theta_i = \frac{2W + (i-1)2W}{k_i}. \tag{32}$$

After statistical summarization of the total length and phase change of each path under different reflection conditions. , we take d=6.5 km, G_r=G_t=15 dBi, and P_t=10 W. Through simulation analysis, it can be seen from Figs. 11 and 12 that the receiving power meets the minimum receiving level value of the aforementioned transceiver system under each reflection condition.

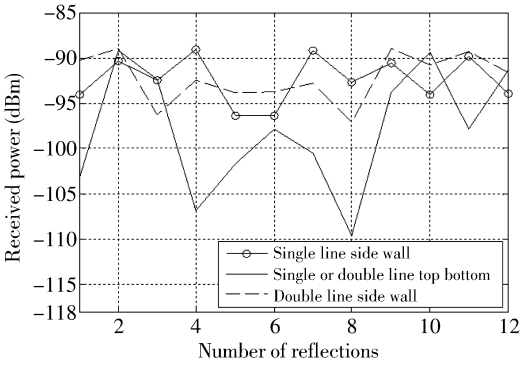

Fig. 11 Received power under single and double line even number reflection

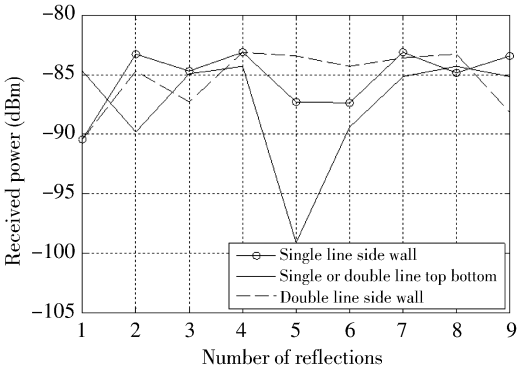

Fig. 12 Received power under single and double line odd number reflection

The propagation environment of dual-line tunnel is more complicated than that of single-line tunnel, especially the reflected wave passes through the top and bottom of the tunnel, resulting in a sharp decrease in the wave power superimposed on the receiving end. Only by adjusting the antenna height and gain value and improving the antenna directivity can the received power fluctuation be alleviated. At the same time, high-speed mobility will cause fast time-varying of multipaths on a small scale. This rapid time-varying phenomenon is reflected in the existence of multipaths at different times and disappears with a certain probability, mainly concentrated on the root mean square delay spread. And the calculated ratio of the total path length to the speed of light is the multipath reception delay, from which the relationship between the delay and the received power can be derived. Our study lays the foundation for further study on the radio waves caused by the multipath delay extension in the T2T tunnel scenario small-scale fading characteristics.

4 Conclusions

1) By analyzing the requirements of T2T technology and combining the spatial distribution of railway operation scenarios, a scheme with a communication distance of 6.5 km and using a 35 GHz millimeter wave in the tunnel to assist communication at 2.8 GHz in the plain region is proposed. At the same time, considering the scattering of millimeter wave caused by rainfall, the scheme is proved feasible by using the principle of large-scale wave propagation.

2) Through the improved Doppler frequency shift calculation equation, the linear relationship between frequency shift and train speed difference under constant speed and acceleration in the interval and station, and the influence of Doppler expansion on the channel are analyzed. Simulation results show that Doppler shift value of T2T low frequency band is significantly lower than the frequency shift value of the train-to-ground communication under the same speed conditions.

3) The ray-tracing method is used to simulate multipath wave, and the simulation analysis shows that under different reflection times, the superimposed multipath signal power at the receiving end meets the minimum receiving level, which can provide a reference for outdoor testing.

References

[1] Ai B, Guan k, Rupp M, et al. Future railway services-oriented mobile communications network. IEEE Journal of Communications Magazine, 2015, 53(10): 78-85.

[2] Shen T, Song H F. A new movement authority based on vehicle-centric communication. Wireless Communications and Mobile Computing, 2018: 1-10.

[3] Lehner A, Strang T, Unterhuber P. Direct train-to-train communications at low UHF frequencies. In: Proceedings of IEEE 11th European Conference on Antennas and Propagation, Paris, 2018: 486-491.

[4] Soliman M, Unterhuber P, Sand S. Dynamic train-to-train propagation measurements in the millimeter wave band-campaign and first results. In: Proceedings of IEEE 13th European Conference on Antennas and Propagation. Poland, 2019: 1-5.

[5] Liu P Y, Ai B, Zhong Z D. A novel train-to-train communication model design based on multihop in high-speed railway. International Journal of Antennas and Propagation, 2012: 1-9.

[6] Chen Q X, Li M Q, Lin J T. Research on train-to-train direct communication technology based on ultrashort wave. Computer Engineering, 2013, 39(12): 5-10.

[7] Unterhuber P, Sand S, Fiebig U, et al. Path loss models for train-to-train communications in typical high speed railway environments. In: Proceedings of IEEE 11th European Conference on Antennas and Propagation. Paris, 2018: 492-500.

[8] Mohammad K M, Karami E, Dobre O A, at el. Doppler spread estimation in MIMO frequency-selective fading channels. Transactions on Wireless Communications, 2018, 17(3): 1951-1965.

[9] He D P, Ai B, Zhong Z D, et al. Channel measurement, simulation and analysis for high-speed railway communications in 5G millimeter wave band. IEEE Transaction on Intelligent Transportation Systems, 2018, 19(10): 3144-3158.

[10] China Railway Corporation. Railway Technology Management Regulations. Beijing: China Railway Press, 2014: 120-135.

[11] Lehner A, Cristina R G, Strang T. On the performance of TETRA DMO short data service in railway VANETs. IEEE Journal of Wireless Personal Communications, 2013, 69(4): 1647-1669.

[12] Feng Y H, Zheng M, Bu Z Y. Wireless channel modeling and simulation in high-speed railway environment. Computer Applications and Software, 2013, 30(3): 96-99.

[13] Dudley D G, Lienard M, Mahmoud S F, et al. Wireless propagation in tunnels. Antennas and Propagation Magazine, 2007 49(2): 11-26.

[14] Fernandez H, Rubio L, Rodrigo-Penarrocha V M, et al. Path loss characterization for vehicular communications at 700&-nbsp; MHz and 5. 9&-nbsp; GHz under LOS and NLOS conditions. IEEE Antennas Wireless Propagation Letters, 2014, 13(1): 931-934 .

[15] Lou K Y. The equation of acoustic wave doppler effect based on relative motion. Physics Teacher, 2013, 34 (10): 90-92.

[16] Dermoune A, Simon E P. Analysis of the maximum likelihood channel estimator for OFDM systems in the presence of unknown interference. Eurasip Journal on Advances in Signal Processing, 2017, 1: 69.

[17] Briso-Rodríguez C, Fratilescu P, Xu Y. Path loss modeling for rrain-to-rrain communications in subway tunnels at 900/2400 MHz. IEEE Antennas and Wireless Propagation Letters, 2019, 18(6): 1164-1168.

[18] Li S J, Li M Q, Gao Y B, et al. Design and performance analysis of multi-band direct communication system between trains. Computer Engineering and Applications, 2017, 53(13): 104-112.

列车对列车无线通信中的信道特性分析

高云波，田智愚，李茂青，岳丽丽，闫丽霞，程　璇

（兰州交通大学 自动化与电气工程学院，甘肃 兰州 730070）

摘　要： 列车对列车(Train-to-train，T2T)通信能为现有车-地专网通信提供保障，其信道特性直接影响上层通信技术的应用。首先，根据铁路运营场景的空间分布结构和菲涅尔带理论提出一种适用于平原和长直隧道场景下追踪列车间直接通信的频率分配方案，并结合由降雨引起电波衰减的估算方法分析多频段无线信道的大尺度衰落。其次，推导 T2T 通信的最大多普勒频移计算公式，并通过射线跟踪法描述隧道内多径波，以分析小尺度衰落。最后，在同等速度条件下，仿真分析得出 T2T 通信低频段最大多普勒频移值明显低于车-地通信频移值。

关键词： 列车对列车通信；菲涅尔带；长直隧道；无线信道；多普勒频移计算

引用格式： GAO Yunbo, TIAN Zhiyu, LI Maoqing, et al. Channel characteristics analysis of train-to-train wireless communication. Journal of Measurement Science and Instrumentation, 2021, 12(3): 331-339. DOI: 10. 3969/j. issn. 1674-8042. 2021. 03. 011